Journal of Sound and Vibration 327 (2009) 109–120

Contents lists available at ScienceDirect

Journal of Sound and Vibration

journal homepage: www.elsevier.com/locate/jsvi

Attenuation and localization of bending waves in a periodic/disordered fourfold composite beam

Zhi-Zhong Yan [a], Chuanzeng Zhang [a,*], Yue-Sheng Wang [b]

[a] Department of Civil Engineering, University of Siegen, D-57068 Siegen, Germany
[b] Institute of Engineering Mechanics, School of Civil Engineering, Beijing Jiaotong University, Beijing 100044, PR China

ARTICLE INFO

Article history:
Received 30 September 2008
Received in revised form
6 June 2009
Accepted 9 June 2009
Handling Editor: C.L. Morfey
Available online 7 July 2009

ABSTRACT

By using the transfer matrix method this paper presents a study of the complex band structure, attenuation spectra and localization of bending waves in a periodic/disordered fourfold composite beam constructed by inserting thin piezoelectric or soft rubber layer at each interface of original elastic composite structures. Numerical examples are presented and the accuracy is validated by the wavelet method. The results show that the piezoelectricity can adjust the band gaps and the soft rubber can enlarge the degree of the localization and the frequency ranges of the complex band gaps. The localization factor resembles the shape of the attenuation curve in the complex band gaps. Subtle differences between the random disorder and the deterministic disorder are observed, except at lower frequencies. The behavior of the wave propagation and localization in random disordered beams can be altered by tuning different inserting position. The existence of piezoelectricity and/or soft rubber layers lends new insight into the vibration control of composite beams.

© 2009 Elsevier Ltd. All rights reserved.

1. Introduction

Recently, the problem of classical such as electromagnetic, acoustic or elastic wave propagation in periodic or disordered structures has received increasing interest [1–13]. Most of these works in literatures focused on the existence of complete elastic/acoustic band gaps within which sound and vibrations are all forbidden in perfectly periodic structures, and on investigating the influences of different geometrical and material parameters on these gaps. In view of applications, more attention should be paid to the attenuation and the localization properties since real periodic structures are usually disordered due to the material defects or the manufacturing errors.

Beams are popular structural elements widely used in many kinds of engineering constructions. Recently, flexural wave propagation in periodic/disordered beams has been investigated both theoretically and experimentally [4–8]. Unlike the non-periodic engineering structures, the periodic ones have many special dynamic characteristics such as pass-bands and stop-bands. Moreover, the disordered periodic structures may exhibit wave and vibration localization. Wave and vibration localization enables us to control and operate the propagation of waves and vibrations and hence has many potential engineering applications such as in acoustic filters, vibration isolation and design of new transducers. On the other hand, wave and vibration localization may lead to local energy concentration which may influence the reliability, durability and the service-life of engineering structures. For this reason, special and anomalous dynamic characteristics of periodic and disordered structures have received considerable attention in recent years. As well known, intelligent materials and

* Corresponding author. Tel.: +49 2717402173; fax: +49 2717404074.
E-mail address: c.zhang@uni-siegen.de (C. Zhang).

0022-460X/$ - see front matter © 2009 Elsevier Ltd. All rights reserved.
doi:10.1016/j.jsv.2009.06.009

structures possess the abilities of self-adaptive and active control. They can perceive the changes of outer environment and properly respond to these changes. Among various intelligent materials, piezoelectric composite materials are more and more widely applied in aeronautic field. Besides, as for the applications in sound or vibration shelter, the size of periodical structures is of crucial importance. Conventional elastic-wave band-gap material operating under the principle of Bragg reflection mechanism can hardly fulfill it because of the long sound wavelength in common elastic solids. The pioneering work of Liu et al. [9] advanced the locally resonant mechanism where very soft rubber was used and showed that narrow gap with low frequency existed. In Refs. [4–7], band gaps have been analyzed by using the Bragg reflection mechanism. In Ref. [8], the bending wave attenuation in a slender beam with periodically attached local resonators has been studied under the local resonance theory illustrated by Liu et al. in their pioneering work [9]. To the knowledge of the authors, only few studies on fourfold composite beams with both piezoelectric and soft rubber layers in disordered periodic structures have been performed. Chen et al. [7] studied the flexural wave localization in a disordered periodic piezoelectric beam and analyzed the effects of several disorder parameters on the localization factor. However, the complex band structure was not calculated in [7] to clarify the physical meaning of the localization factor in a direct way. Moreover, the locally resonant mechanism which may lead to novel wave localization phenomenon was not considered in [7].

In this paper, in order to find the key function of piezoelectricity and soft rubber to give better design guidelines for flexural wave attenuation of slender composite beams, a comprehensive study of the attenuation and localization of bending waves in periodic/disordered beams is presented, where the effects of both the piezoelectric and the soft rubber layers are considered. In the composite beams investigated in this paper, thin piezoelectric or soft rubber layers are periodically inserted at each interface of the original composite beams. A concise presentation of the transfer matrix (TM) theory for layered slender beams is given. Then it is validated with the wavelet (WL) method [10], and the expression of the localization factor is presented. Numerical examples are given and the influences of the piezoelectric or soft rubber layers on the complex band structures of the periodic composite beams are analyzed. In addition, disorders of the piezoelectric or soft rubber layers in different inserting position are investigated and discussed. Some design instructions in view of the applications are drawn from the present study as conclusions.

2. Transfer matrix method for composite beams

A schematic sketch of a periodic fourfold composite structure studied in the paper is shown in Fig. 1. It is constructed by inserting continuously thin piezoelectric or soft rubber layers at each interface of the original composite beam which is composed of two different elastic materials. The local coordinates of each monolayer are also given in this figure. Assuming that the lengths of the monolayers are a_i $(i = 1, 2, \ldots, 4)$, respectively, and the beam length between the two consecutive unit cells or the so-called lattice constant is a.

For a slender beam as shown in Fig. 1, the equations of wave motion in the elastic and the piezoelectric layers can be expressed, respectively as follows [7]

$$E_l I_l u_l^{\mathrm{IV}} + \rho_l A \ddot{u}_l = 0, \tag{1}$$

$$E_r I_r u_r^{\mathrm{IV}} + E_r I_r b u_r'' + \rho_r A \ddot{u}_r = 0, \tag{2}$$

where u_l and u_r are the displacements in the y-direction, E_l and E_r the Young's moduli, I_l and I_r the moments of inertia with respect to the axis perpendicular to the beam axis, and ρ_l and ρ_r the mass densities with l referring to the elastic beams and r to the piezoelectric beams; A is the area of the cross-section; $b = -e_{31}e_{15}A/\varepsilon_{11}E_r I_r$ with e_{31}, e_{15} and ε_{11} being the piezoelectric constants and the dielectric constant; the superscript IV denotes the fourfold spatial derivatives; and double dots over a quantity stand for temporal derivatives. By considering the normal-mode condition and assuming the time-harmonic solution the displacements may be written as

$$u_l(x_l, t) = U_l(x_l)\ \exp(-\mathrm{i}\omega t), \tag{3}$$

$$u_r(x_r, t) = U_r(x_r)\ \exp(-\mathrm{i}\omega t), \tag{4}$$

where $\mathrm{i} = \sqrt{-1}$; ω is the circular frequency; and $U_l(x_l)$ and $U_r(x_r)$ are the amplitudes of the displacements.

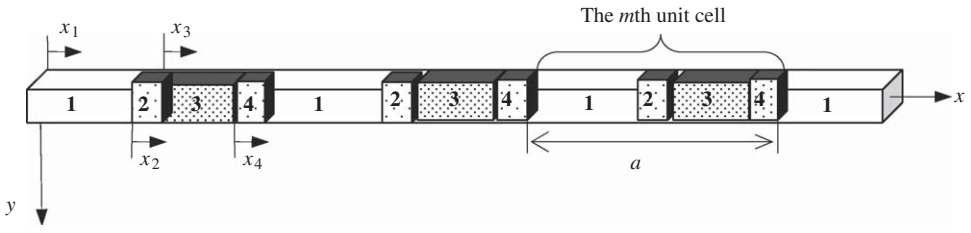

Fig. 1. A beam periodically inserted with piezoelectric or soft rubber layers at each interface.

With substitution of Eqs. (3) and (4) into Eqs. (1) and (2), the solutions of Eqs. (1) and (2) for the displacement amplitudes of the beam can be written as

$$U_l = A_{l1}\cosh(S_l\eta_l) + A_{l2}\sinh(S_l\eta_l) + A_{l3}\cos(S_l\eta_l) + A_{l4}\sin(S_l\eta_l), \tag{5}$$

$$U_r = B_{r1}\cosh(S_r\eta_r) + B_{r2}\sinh(S_r\eta_r) + B_{r3}\cos(S_{r+1}\eta_r) + B_{r4}\sin(S_{r+1}\eta_r), \tag{6}$$

where

$$S_l = \sqrt[4]{\rho_l A\omega^2/E_l I_l}a_0, \quad S_r = \sqrt{\sqrt{\rho_r A\omega^2/E_r I_r + b^2/4} - b/2}a_0,$$

$$S_{r+1} = \sqrt{\sqrt{\rho_r A\omega^2/E_r I_r + b^2/4} + b/2}a_0, \tag{7}$$

$\eta_l = x_l/a_0$ and $\eta_r = x_r/a_0$ are the normalized local coordinates, with a_0 being the mean value of the lengths of the elastic beams. In Eqs. (5) and (6), A_{lk} and B_{rk} ($k = 1,2,3,4$) are the unknown coefficients to be determined by the boundary conditions.

Applying the continuity conditions of the displacements, slopes, bending moments and shear forces at the left and the right sides of each monolayer in the mth unit cell, one can obtain, for the left coefficients vector

$$\psi_{lL}^{(m)} = \{U_{lL}^{(m)}, \theta_{lL}^{(m)}, \bar{O}_{lL}^{(m)}, \bar{T}_{lL}^{(m)}\}^{\mathrm{T}} \tag{8}$$

and the right coefficients vector

$$\psi_{lR}^{(m)} = \{U_{lR}^{(m)}, \theta_{lR}^{(m)}, -\bar{O}_{lR}^{(m)}, \bar{T}_{lR}^{(m)}\}^{\mathrm{T}} \tag{9}$$

of the elastic monolayers in the mth unit cell, the following relation

$$\psi_{lR}^{(m)} = \mathbf{T}_l'\psi_{lL}^{(m)}. \tag{10}$$

In Eq. (10), $\mathbf{T}_l'$ is the transfer matrix which is defined by

$$\mathbf{T}_l' = \mathbf{P}_l'\mathbf{P}_l^{-1},$$

where the matrices $\mathbf{P}_l$ and $\mathbf{P}_l'$ can be written as

$$\mathbf{P}_l = \begin{bmatrix} 1 & 0 & 1 & 0 \\ 0 & S_l & 0 & S_l \\ -S_l^2 & 0 & S_l^2 & 0 \\ 0 & S_l^3 & 0 & -S_l^3 \end{bmatrix}, \tag{11}$$

$$\mathbf{P}_l' = \begin{bmatrix} \cosh(S_l d_l^{(m)}) & \sinh(S_l d_l^{(m)}) & \cos(S_l d_l^{(m)}) & \sin(S_l d_l^{(m)}) \\ S_l\sinh(S_l d_l^{(m)}) & S_l\cosh(S_l d_l^{(m)}) & -S_l\sin(S_l d_l^{(m)}) & S_l\cos(S_l d_l^{(m)}) \\ -S_l^2\cosh(S_l d_l^{(m)}) & -S_l^2\sinh(S_l d_l^{(m)}) & S_l^2\cos(S_l d_l^{(m)}) & S_l^2\sin(S_l d_l^{(m)}) \\ S_l^3\sinh(S_l d_l^{(m)}) & S_l^3\cosh(S_l d_l^{(m)}) & S_l^3\sin(S_l d_l^{(m)}) & -S_l^3\cos(S_l d_l^{(m)}) \end{bmatrix}. \tag{12}$$

Here, $d_l = a_l/a_0$ is the dimensionless length of each elastic monolayer; θ_m, O_m and T_m represent the rotation angle, moment and shear force, respectively; and the subscripts L and R denote the left and the right sides of the elastic monolayers in the mth unit cell.

Similarly, we obtain for the piezoelectric layer

$$\psi_{rR}^{(m)} = \mathbf{T}_r'\psi_{rL}^{(m)}, \tag{13}$$

where the transfer matrix $\mathbf{T}_r'$ is defined by

$$\mathbf{T}_r' = \mathbf{P}_r'\mathbf{P}_r^{-1}, \tag{14}$$

in which the matrices $\mathbf{P}_r$ and $\mathbf{P}_r'$ are given by

$$\mathbf{P}_r = \begin{bmatrix} 1 & 0 & 1 & 0 \\ 0 & S_r & 0 & S_{r+1} \\ -S_r^2 & 0 & S_{r+1}^2 & 0 \\ 0 & S_r^3 & 0 & -S_{r+1}^3 \end{bmatrix}, \tag{15}$$

$$\mathbf{P}'_r = \begin{bmatrix} \cosh(S_r d_r^{(m)}) & \sinh(S_r d_r^{(m)}) & \cos(S_{r+1} d_r^{(m)}) & \sin(S_{r+1} d_r^{(m)}) \\ S_r \sinh(S_r d_r^{(m)}) & S_r \cosh(S_r d_r^{(m)}) & -S_{r+1} \sin(S_{r+1} d_r^{(m)}) & S_{r+1} \cos(S_{r+1} d_r^{(m)}) \\ -S_r^2 \cosh(S_r d_r^{(m)}) & -S_r^2 \sinh(S_r d_r^{(m)}) & S_{r+1}^2 \cos(S_{r+1} d_r^{(m)}) & S_{r+1}^2 \sin(S_{r+1} d_r^{(m)}) \\ S_r^3 \sinh(S_r d_r^{(m)}) & S_r^3 \cosh(S_r d_r^{(m)}) & S_{r+1}^3 \sin(S_{r+1} d_r^{(m)}) & -S_{r+1}^3 \cos(S_{r+1} d_r^{(m)}) \end{bmatrix}. \tag{16}$$

Considering the following relationships

$$\psi_{1L}^{(m+1)} = \mathbf{W}_{\kappa 1} \psi_{4R}^{(m)}, \quad \psi_{4R}^{(m)} = \mathbf{T}'_{\kappa 4} \psi_{4L}^{(m)}, \quad \psi_{4L}^{(m)} = \mathbf{W}_{\kappa 2} \psi_{3R}^{(m)}, \quad \psi_{3R}^{(m)} = \mathbf{T}'_{\kappa 3} \psi_{3L}^{(m)},$$

$$\psi_{3L}^{(m)} = \mathbf{W}_{\kappa 3} \psi_{2R}^{(m)}, \quad \psi_{2R}^{(m)} = \mathbf{T}'_{\kappa 2} \psi_{2L}^{(m)}, \quad \psi_{2L}^{(m)} = \mathbf{W}_{\kappa 4} \psi_{1R}^{(m)}, \quad \psi_{1R}^{(m)} = \mathbf{T}'_{\kappa 1} \psi_{1L}^{(m)}, \tag{17}$$

we obtain the following equation for the $(m+1)$th unit cell

$$\psi_{1L}^{(m+1)} = \mathbf{W}_{\kappa 1} \cdot \mathbf{T}'_{\kappa 4} \cdot \mathbf{W}_{\kappa 2} \cdot \mathbf{T}'_{\kappa 3} \cdot \mathbf{W}_{\kappa 3} \cdot \mathbf{T}'_{\kappa 2} \cdot \mathbf{W}_{\kappa 4} \cdot \mathbf{T}'_{\kappa 1} \cdot \psi_{1L}^{(m)} = \mathbf{T}_m \psi_{1L}^{(m)}, \tag{18}$$

where the elements of the matrix $\mathbf{W}_{\kappa j}$ ($\kappa = l, r$; $j = 1,2,3,4$) can be written as

$$\mathbf{W}_{\kappa 1} = \begin{bmatrix} 1 & 0 & 0 & 0 \\ 0 & 1 & 0 & 0 \\ 0 & 0 & E_4/E_1 & 0 \\ 0 & 0 & 0 & E_4/E_1 \end{bmatrix}, \quad \mathbf{W}_{\kappa 2} = \begin{bmatrix} 1 & 0 & 0 & 0 \\ 0 & 1 & 0 & 0 \\ 0 & 0 & E_3/E_4 & 0 \\ 0 & 0 & 0 & E_3/E_4 \end{bmatrix}, \tag{19}$$

$$\mathbf{W}_{\kappa 3} = \begin{bmatrix} 1 & 0 & 0 & 0 \\ 0 & 1 & 0 & 0 \\ 0 & 0 & E_2/E_3 & 0 \\ 0 & 0 & 0 & E_2/E_3 \end{bmatrix}, \quad \mathbf{W}_{\kappa 4} = \begin{bmatrix} 1 & 0 & 0 & 0 \\ 0 & 1 & 0 & 0 \\ 0 & 0 & E_1/E_2 & 0 \\ 0 & 0 & 0 & E_1/E_2 \end{bmatrix}. \tag{20}$$

In Eq. (18), $\mathbf{T}_m$ is the transfer matrix between the two consecutive unit cells.

As for a randomly disordered beam, the localization factor can be used to describe the wave propagation and localization effectively [11]. The localization factor is defined by the smallest positive Lyapunov-exponent χ_d and is given by

$$\chi_d = \lim_{n\to\infty} \frac{1}{n} \sum_{m=1}^{n} \ln \|\hat{\psi}_{4R,d}^{(m)}\|, \tag{21}$$

where

$$\hat{\psi}_{4R,d}^{(m)} = \psi_{4R,d}^{(m)} - (\psi_{4R,d}^{(m)}, \mathbf{v}_{d-1}^{(m)}) \mathbf{v}_{d-1}^{(m)} - \cdots - (\psi_{4R,d}^{(m)}, \mathbf{v}_1^{(m)}) \mathbf{v}_1^{(m)}, \quad \mathbf{v}_d^{(m)} = \frac{\hat{\psi}_{4R,d}^{(m)}}{\|\hat{\psi}_{4R,d}^{(m)}\|}. \tag{22}$$

In Eq. (22), $\mathbf{v}_d^{(m)}$ are orthogonal unit vectors; $(\cdot,\cdot)$ denotes the dot-product; and n represents the number of unit cells of the periodic structures.

3. Numerical results and discussions

In this section, numerical simulation for periodic/disordered elastic and piezoelectric composite structures is performed to study the behavior of the attenuation and localization of bending waves with different frequencies. The used material constants are listed in Table 1.

Table 1
Material constants of the elastic and piezoelectric layers.

Materials	Mass density ρ (kg/m^3)	Young's modulus E (Pa)	Piezoelectric constant (C/m^2)		Dielectric constants ε_{11} (10^{-10} F/m)
			e_{31}	e_{15}	
Pb	11600	4.07×10^{10}			
Epoxy	1180	4.3×10^{9}			
Rubber	1300	1.13×10^{5}			
PZT-5H	7500	12.6×10^{10}	−6.5	17.44	150.3

3.1. The complex band structure and localization in a perfectly periodic beam

First, we consider a perfectly periodic beam consisting of two different elastic materials Pb and Epoxy alternately. Then, we investigate the influences of thin piezoelectric and soft rubber layers on the propagation and localization of bending waves by inserting them at each interface of the composite beam. For comparison purpose, the length ratio of the Pb and Epoxy layers or beams is fixed as $a_{Pb}/a_{Epoxy} = 2$ and the same material, i.e., either PZT-5H or rubber, is inserted to the composite beam.

For three kinds of perfectly periodic composite structures, i.e., Pb–Epoxy, Pb–PZT–Epoxy–PZT and Pb–Rubber–Epoxy–Rubber composites, Figs. 2–4 show the complex band structure, the attenuation and the localization factor of bending waves. For convenience, a dimensionless frequency is introduced as $\omega a_{Epoxy}/c_{T,Epoxy}$, where $c_{T,Epoxy}$ denotes the shear wave velocity of Epoxy. The localization factors are illustrated in the Figs. 2–4(a), while Figs. 2–4(b) present the real wavenumber and Figs. 2–4(c) show the absolute value of the imaginary part of the wavenumber, in which the solid circles and the dashed lines denote the propagating and near-field wave components as discussed in Ref. [12], respectively. It can be observed from these figures that perfectly periodic structures have the properties of frequency pass-bands and stop-bands or band gaps. For example, as seen in Fig. 2(a) by the solid lines, the frequency interval $\omega a_{Epoxy}/c_{T,}$ Epoxy $\in (0.12, 0.18)$, in which the localization factors are zero, is called the pass-band, and the interval $\omega a_{Epoxy}/c_{T,Epoxy} \in (0.18, 0.28)$ is known as the stop-band or band gap, in which the localization factors are larger than zero in the considered frequency range. Fig. 2(b) shows a comparison of the band structures of the composite beam obtained by the transfer matrix method and the wavelet method [10], which is described briefly in the Appendix A. It can be seen that they are in very good agreement and the

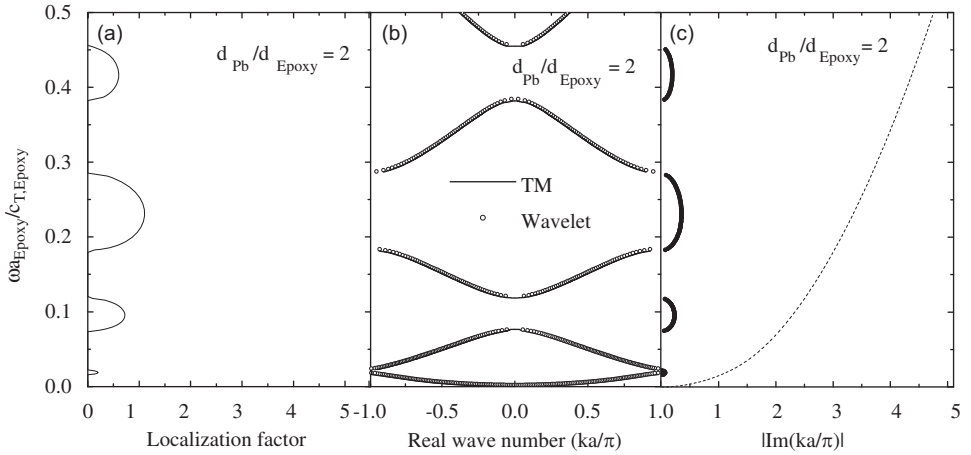

Fig. 2. The complex band structure of the binary composite beam, the localization factor and the attenuation: (a) localization factor; (b) real wavenumber; (c) the absolute value of the imaginary part of complex wavenumber. The solid circles and dashed lines denote the propagating and the near-field waves, respectively.

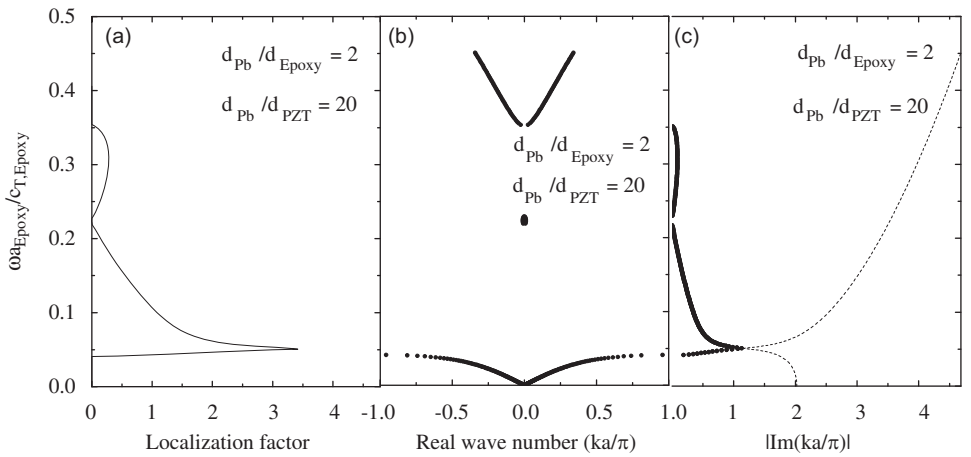

Fig. 3. The complex band structure of a fourfold composite beam with piezoelectric layers, the localization factor and the attenuation: (a) localization factor; (b) real wavenumber; (c) the absolute value of the imaginary part of complex wavenumber. The solid circles and dashed lines denote the propagating and the near-field waves, respectively.

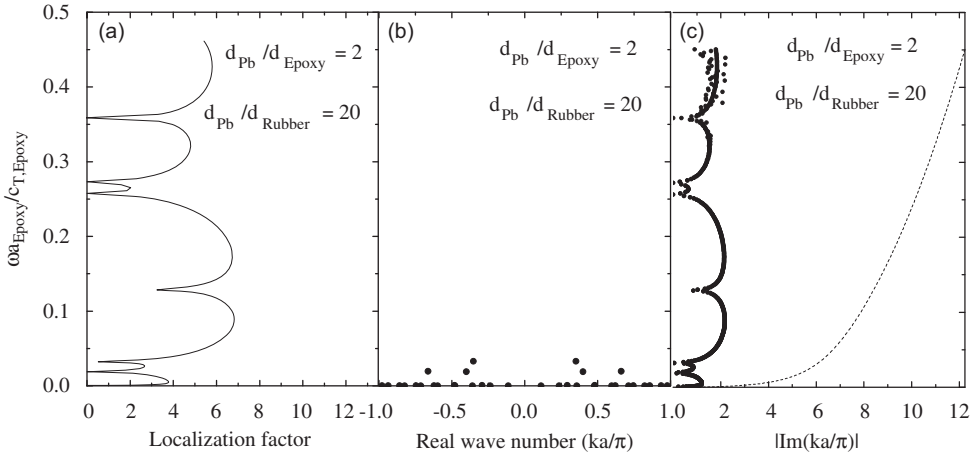

Fig. 4. The complex band structure of a fourfold composite beam with rubber layers, the localization factor and the attenuation; (a) localization factor; (b) real wavenumber; (c) the absolute value of the imaginary part of complex wavenumber. The solid circles and dashed lines denote the propagating and the near-field waves, respectively.

accuracy of the transfer matrix method is therefore validated. Moreover, the band structure of Fig. 2(b) has pass-bands and stop-bands exactly in the same frequency range of Fig. 2(a), which validate each other. It can also be seen that the shape of the attenuation curve described by the solid circles in Fig. 2(c) strongly resembles the localization factor in Fig. 2(a), which implies that the localization factor can be used to describe the attenuation properties in the band gaps. However, there are some differences between Figs. 4(a) and (c) at higher frequencies, which means that the localization factor only characterizes the "average" exponential rate of decay of the wave amplitudes. It can also be seen that the attenuation curve (solid circles) shown in Fig. 3(c) has a peak, which means that the attenuation is the strongest at the low frequency end of the gap and it becomes weaker with increase of the frequency. This resembles the Fano-like interference phenomena in phononic crystals with locally resonant structures [14].

From Figs. 2–4, we can also see that for different composite beams the complex band structures and the localization factors have obvious changes. In these figures, the behaviors of the band structures (for instance near $\omega a_{\mathrm{Epoxy}}/c_{\mathrm{T,Epoxy}} = 0.1$) are notably different, which means that the piezoelectric and the soft rubber layers have significant effects on the band structures although their length is only 1/10th of the length of the Epoxy layer.

The amplitudes of the displacement $|u(x)|$ associated with the frequency bands for Pb–Epoxy and Pb–PZT–Epoxy–PZT composite beams are presented in Fig. 5. The band-edge frequency $\omega a_{\mathrm{Epoxy}}/c_{\mathrm{T,Epoxy}} = 0.01683$ corresponds to the boundary mode frequency in Fig. 5(a) which is discussed in [13]. The boundary mode is associated with as an increase in the displacement towards the end of the Pb layer in one period. The curves for $\omega a_{\mathrm{Epoxy}}/c_{\mathrm{T,Epoxy}} = 0.0021$ outside the band gap correspond to a vibration mode, and elastic waves can propagate at this frequency. In contrast, the curves for $\omega a_{\mathrm{Epoxy}}/c_{\mathrm{T,Epoxy}} = 0.2385$ inside the band gap correspond to vibration isolation, and the propagation of elastic waves is prohibited at this frequency. It can also be seen that the amplitude of the displacement within the thin piezoelectric layers abruptly drops, which shows that the piezoelectric layer has obvious effects on the displacement of the composite beam.

Similarly, the amplitudes of the displacement $|u(x)|$ associated with the frequency bands for Pb–Epoxy and Pb–Rubber–Epoxy–Rubber composite beams are shown in Fig. 6. The curves for $\omega a_{\mathrm{Epoxy}}/c_{\mathrm{T,Epoxy}} = 0.00071329$ outside the band gap correspond to a vibration mode at which elastic waves can propagate. In contrast to this, the curves for $\omega a_{\mathrm{Epoxy}}/c_{\mathrm{T,Epoxy}} = 0.2385$ inside the band gap correspond to vibration isolation, and elastic waves cannot propagate at this frequency. It can also be seen that the amplitude of the displacement within the thin rubber layers jumps and becomes larger because the mass of rubber layer is much smaller than Pb and Epoxy layers at the same thickness.

In the following examples, we consider the effects of the elastic layers or beams (Pb, Epoxy) and inserted piezoelectric or rubber disorders. Five kinds of length disorders are considered, i.e., the length a_1 (Pb), the length a_2 ($\mathrm{PZT_{left}}$, $\mathrm{Rubber_{left}}$), the length a_3 (Epoxy) and the length a_4 ($\mathrm{PZT_{right}}$, $\mathrm{Rubber_{right}}$) of the piezoelectric or rubber layers, and both (Pb+Epoxy, $\mathrm{PZT_{left+right}}$, $\mathrm{Rubber_{left+right}}$) disorders simultaneously. For the randomly disordered beam, a random parameter L denoting a_1, a_2, a_3 or a_4 is introduced. Here, L is assumed to be a uniformly distributed random variable with the mean value L_0 and the variation coefficient δ. So L is a random variable in the interval

$$L \in [L_0(1-\sqrt{3}\delta), L_0(1+\sqrt{3}\delta)]. \tag{23}$$

Introducing a standard uniformly distributed random variable $t \in (0,1)$, then L can be expressed as

$$L = L_0[1+\sqrt{3}\delta(2t-1)]. \tag{24}$$

It should be noted here that the assumption of uniformly distributed disorders or uniformly distributed random variables L and t is made in this analysis arbitrarily just for simplicity, although the method presented in this paper is applicable to

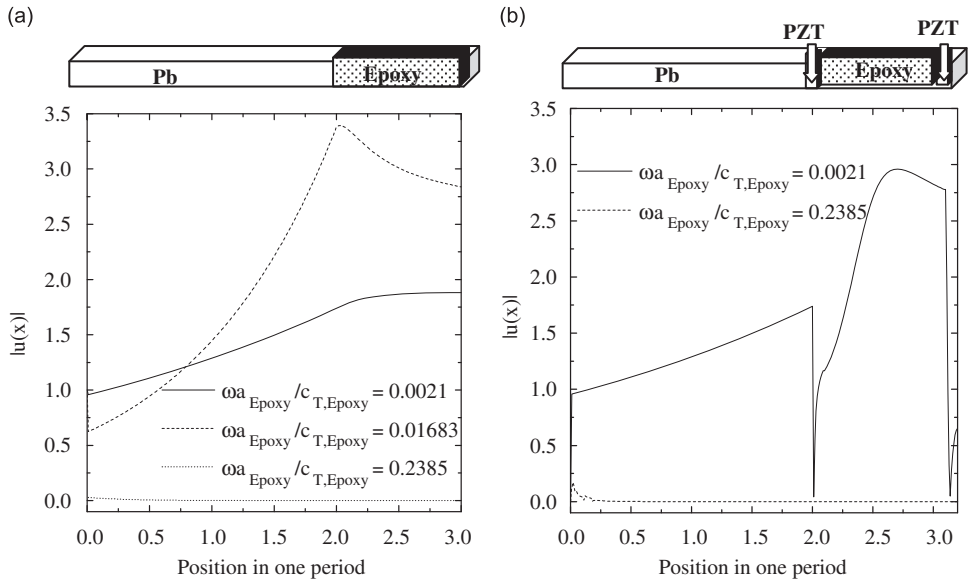

Fig. 5. The amplitude of the displacement as a function of the spatial position.

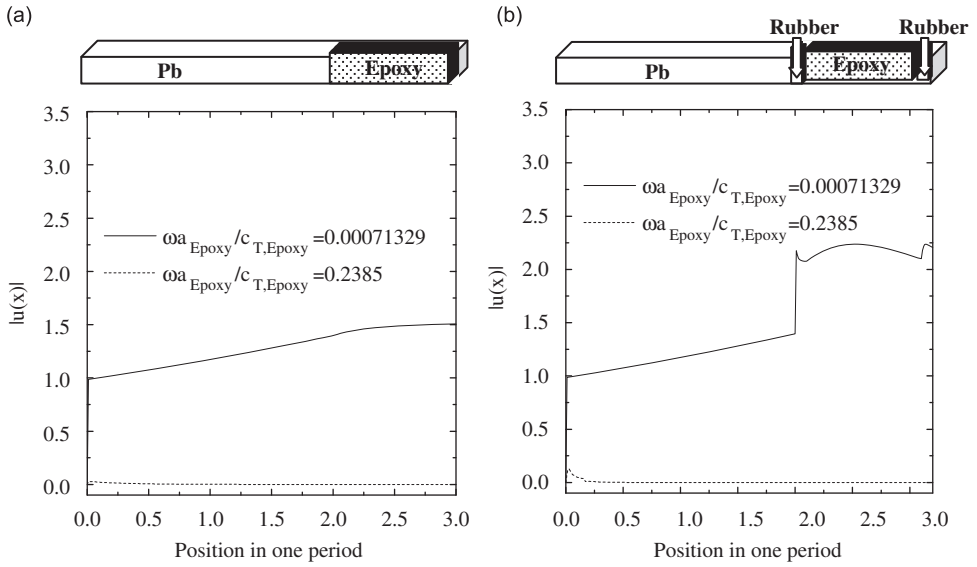

Fig. 6. The amplitude of the displacement as a function of the spatial position.

any kind of random distributions when their statistical information is available. Indeed, according to the central limit theorem, one would expect that normally distributed disorders are the typical situation in practical applications, where a large number of independent stochastic variables occur. On the other hand, uniformly distributed disorders represent the simplest case in practical applications which are hence often assumed in similar analyses.

3.2. Disorder in the length of the elastic layers (Pb, Epoxy) with piezoelectric layers

For the comparison purpose with Ref. [7], it is assumed that $a_1 = 2a_2 = 2a_3 = 2a_4$, that is to say, the length of the piezoelectric layer is half of the Pb layer. For the Pb–PZT–Epoxy–PZT system, the variations of the localization factor with the dimensionless frequency for some selected values of δ are shown in Fig. 7. Similar phenomenon as shown in Fig. 3 of Ref. [7] is observed here. For example, Fig. 7(a) implies that in the interval of $\omega a_{\text{Epoxy}}/c_{\text{T,Epoxy}} \in (0.146, 0.246)$ the localization factor is zero for the case of $\delta = 0$ and this frequency interval is a pass-band. But in this pass-band the

localization factor is positive in the case of $\delta \neq 0$, i.e., the localization phenomenon appears. Moreover, with the increase of the variation coefficient δ, the localization factor is no longer zero in the pass-bands and the degree of the localization increases. On the other hand, in the interval of $\omega a_{\mathrm{Epoxy}}/c_{\mathrm{T,Epoxy}} \in (0.25, 0.33)$ the localization factor is positive and this interval is known as a stop-band. In general, in the stop-band the localization factor of the random structure ($\delta \neq 0$) is less than that of the corresponding periodic structure ($\delta = 0$). From Fig. 7, it can also be seen that the localization behaviors are different for various disorders of the elastic layers. For instance, in the high frequency range the localization factor for Epoxy disorders is much smaller than that for Pb disorders or a combination of Pd and Epoxy disorders. This example shows that the localization behavior depends on the disorder type of the elastic layers in each unit cell.

3.3. Disorder in the length of the piezoelectric layers at different location

For three kinds of disordered periodic piezoelectric composite structures, assume that $a_1 = 2a_2 = 2a_3 = 2a_4$, Fig. 8 shows the variations of the localization factor versus the dimensionless frequency for $\delta = 0$, 0.05 and 0.1. It is observed that similar localization phenomenon as shown in Fig. 7 can occur in the case of piezoelectric disorders. For example, Fig. 8(a) shows that for disordered piezoelectric layers the localization factor is non-zero but positive in the frequency pass-bands of the corresponding tuned periodic structures, i.e., in the interval $\omega a_{\mathrm{Epoxy}}/c_{\mathrm{T,Epoxy}} \in (0.146, 0.246)$, which means that the phenomenon of wave localization occurs. Comparing Fig. 7 with Fig. 8 it can be concluded that the localization induced by a disorder in the length a_4 of the piezoelectric layers as given in Fig. 8(b) is more obvious than that induced by a disorder in the length a_3 of the Epoxy layers as shown in Fig. 7(b) at lower frequencies, i.e., in the first pass-band, and vise versa at

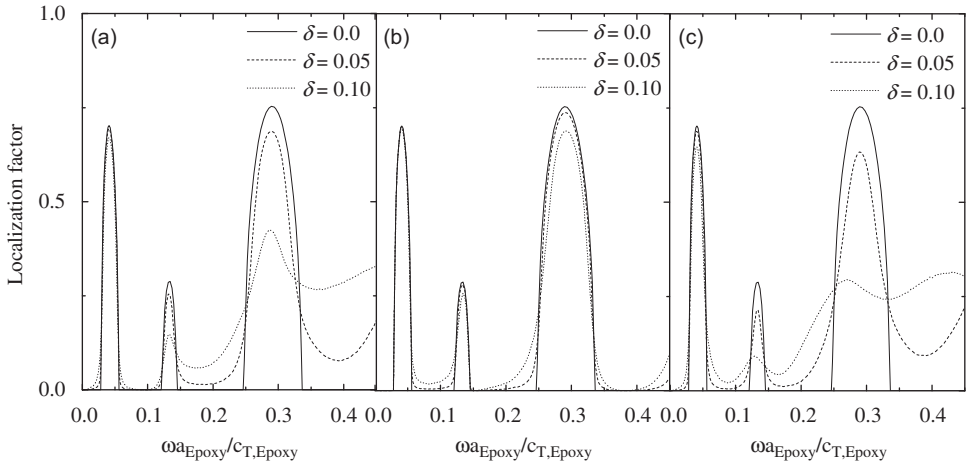

Fig. 7. The localization factors versus the dimensionless frequency for disordered Pb and Epoxy layers with piezoelectric layers: (a) Pb disorder; (b) Epoxy disorder; (c) Pb and Epoxy disorders.

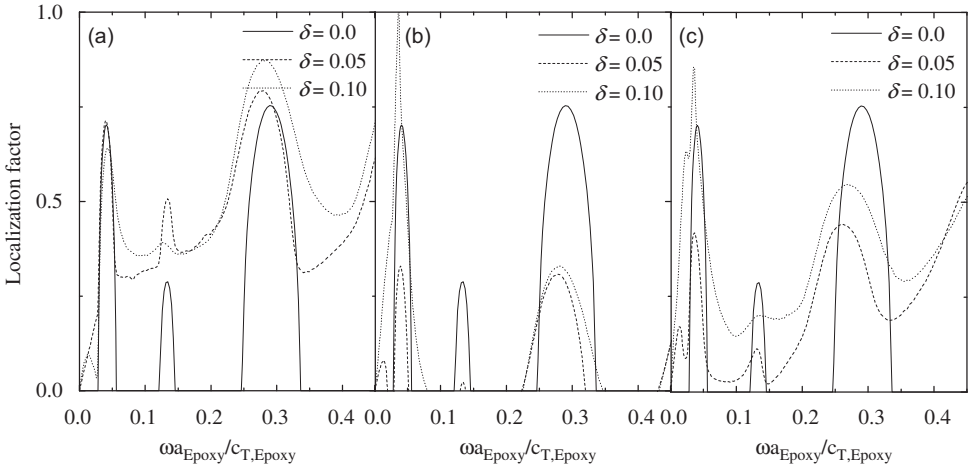

Fig. 8. The localization factors versus the dimensionless frequency for piezoelectric disorders: (a) disorder in a_2; (b) disorder in a_4; (c) disorder in a_2 and a_4.

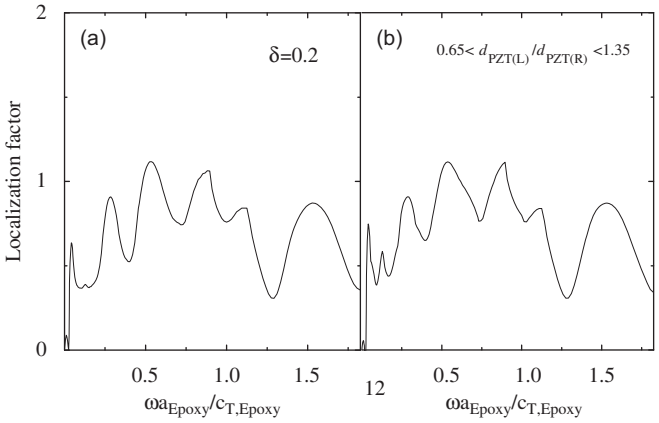

Fig. 9. The localization factors for random and deterministic piezoelectric disorders.

higher frequencies. Furthermore, the localization induced by a disorder in the lengths a_2 and a_2+a_4 of the piezoelectric layers as shown in Figs. 8(a) and (c) is more noticeable than that induced by a disorder in the lengths a_1 and a_1+a_3 of the elastic layers as presented in Figs. 7(a) and (c)) at all frequencies considered, which was not found in binary cases [7] before. Moreover, in the stop-band the localization factor of the random structure ($\delta \neq 0$) may be larger than that of the corresponding periodic structure ($\delta = 0$) at some frequencies, for instance in the frequency interval $\omega a_{Epoxy}/c_{T,Epoxy} \in (0.12, 0.14)$ of Fig. 8(a), which is quite different from that of Fig. 7.

It can also be seen from Fig. 8 that for different disordered periodic piezoelectric composites the behaviors of wave localization are distinct. For example, in the first stop-band the localization factors in Figs. 8(a) and (b) as well as Figs. 8(a) and (c) are rather different. The degree of the wave localization of Fig. 8(b) is strongest among them. Also, the localization degree in the second and the third stop-bands of Fig. 8(a) is much larger than those of Figs. 8(b) and (c), which means that the location of the piezoelectric disorders has significant effects on the wave localization.

Next, we investigate the difference between a random disorder and a deterministic disorder by assuming that a_2 randomly and deterministically changes. According to Eq. (23), a variation coefficient $\delta = 0.2$ corresponds to $0.65L_0 < L < 1.35L_0$. Here, as a random disorder, we change a_2 by introducing a standard uniformly distributed random variable $t \in (0, 1)$ in Eq. (24), while, as a deterministic disorder, we increase a_2 with fixed step-length in the range of $0.65L_0 < L < 1.35L_0$. In Fig. 9, the left figure shows the localization factor for a random disorder while the right figure presents that for a deterministic disorder. It can be seen from Fig. 9 that in the considered case the localization factor for a random disorder is similar to that for a deterministic disorder at most frequencies except at lower frequencies and at least in the considered cases.

3.4. Disorder in the length of the elastic layers (Pb, Epoxy) with rubber layers

Now we consider disorders in the length of the elastic layers (Pb, Epoxy) with thin rubber layers and assume $a_1 = 2a_3 = 20a_2 = 20a_4$. Fig. 10 shows the variations of the localization factor versus the dimensionless frequency for $\delta = 0$, 0.05 and 0.1. It is observed here that similar localization phenomenon as shown in Fig. 7 can occur in the case of Pb, Epoxy or both disorders simultaneously in disordered periodic composite structures with thin rubber layers. By comparing Fig. 10 with Fig. 7 it can be seen that the existence of the soft rubber layers enlarge the band gaps and the degree of the localization. It can also be seen from these figures that there are little differences between Figs. 10(a) and (c). However, in Fig. 10(b), the localization behavior is quite different from that in Figs. 10(a) and (c), which shows that the Pb and Epoxy disorders at different position may have remarkable effects on the localization behaviors.

3.5. Disorder in the length of the rubber layers at different location

Assume $a_1 = 2a_3 = 20a_2 = 20a_4$, Fig. 11 displays the variations of the localization factor versus the dimensionless frequency for $\delta = 0$, 0.05 and 0.1. Here, only slight differences between Figs. 11(a) and (b) are noted. However, in the frequency range $\omega a_{Epoxy}/c_{T,Epoxy} \in (0.2, 0.4)$ the degree of the wave localization in the case of Fig. 11(c) is stronger than that of Figs. 11(a) and (b). A comparison of Fig. 11 with Fig. 10 shows that the localization induced by a disorder in the length of the rubber layers (see Fig. 11) is more perceivable than that induced by a disorder in the length of the elastic layers (see Fig. 10) at lower frequencies. Besides, the localization induced by a disorder in the lengths a_2 and a_2+a_4 of the rubber layers as shown in Figs. 11(a) and (c) is less noticeable than that induced by a disorder in the length a_1 and a_1+a_3 of the elastic layers as shown in Figs. 10(a) and (c) at higher frequencies. However, a disorder in the length a_4 of the rubber layers as

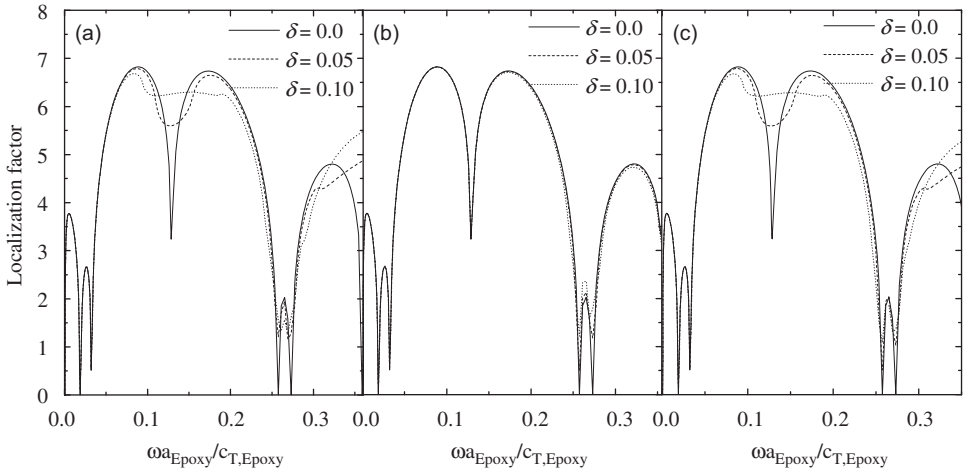

Fig. 10. The localization factors versus the dimensionless frequency for disordered Pb and Epoxy layers with rubber layers: (a) Pb disorder; (b) Epoxy disorder; (c) Pb and Epoxy disorders.

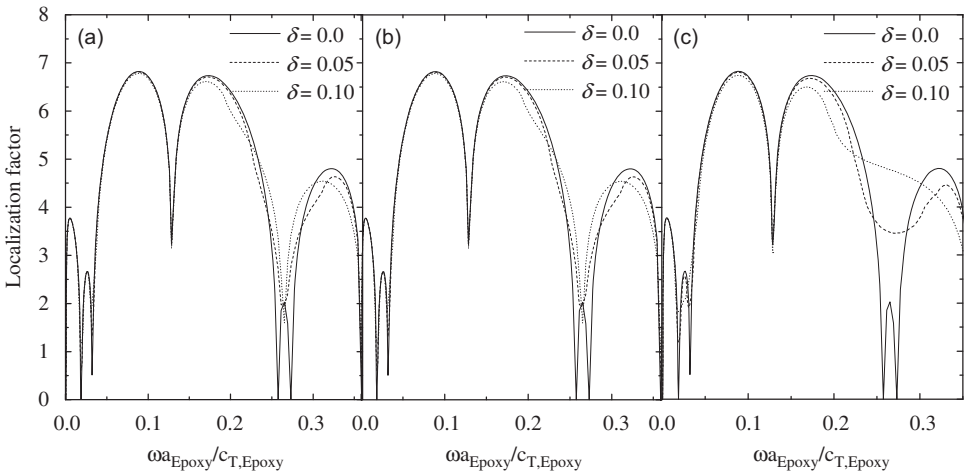

Fig. 11. The localization factors versus the dimensionless frequency for rubber disorders: (a) disorder in a_1; (b) disorder in a_3; (c) disorder in a_1 and a_3.

shown in Fig. 11(b) or in the length a_3 of the elastic layers as given in Fig. 10(b) has similar effects on the wave propagation and localization in the same range of higher frequencies.

4. Conclusions

In this paper, the influences of thin piezoelectric and soft rubber layers on the complex band structures and the localization of bending waves in a periodic/disordered composite beam are investigated. The transfer matrix method is applied for this purpose. The following conclusions can be drawn from this analysis:

- For the perfectly periodic structures, the piezoelectric layers can adjust the band gaps and the soft rubber layers can enlarge the frequency range and the attenuation coefficient in complex band structures. The localization factor resembles the shape of the attenuation curve in the complex band gaps.
- The effects of a random disorder and a deterministic disorder on the localization factor are quite similar except at lower frequencies and at least for the considered cases in this paper.
- For disordered piezoelectric layers, the localization induced by a disorder in the length a_4 of the piezoelectric layers is more obvious than that induced by a disorder in the length a_3 of the elastic layers at lower frequencies, i.e., in the first pass-band, and vise versa at higher frequencies. Besides, the localization induced by a disorder in the lengths a_2 and a_2+a_4 of the piezoelectric layers is more perceivable than that induced by a disorder in the lengths a_1 and a_1+a_3 of the

elastic layers at all considered frequencies. Moreover, in the stop-band the localization factor of the random structure ($\delta \neq 0$) is larger than that of the corresponding periodic structure ($\delta = 0$) at certain frequencies.

- For disordered rubber layers, the localization induced by a disorder in the length of the rubber layers is more remarkable than that induced by a disorder in the length of the elastic layers at lower frequencies. Moreover, the localization induced by a disorder in the lengths a_2 and a_2+a_4 of the rubber layers is less obvious than that induced by a disorder in the lengths a_1 and a_1+a_3 of the elastic layers at higher frequencies. However, a disorder in the length a_4 of the rubber layers or in the length a_3 of the elastic layers has similar effects on the wave propagation and localization in the same range of higher frequencies.
- The behavior of the wave propagation and localization in disordered composite beams can be altered by adjusting elastic disorders at different position or placing thin piezoelectric or soft rubber layers at different inserting location. Thus, desirable wave propagation and localization behaviors can be achieved by properly designing disordered periodic composite structures with thin piezoelectric or soft rubber layers at suitable inserting positions.

Acknowledgments

Support by the German Research Foundation (DFG, Project-no. ZH 15/11-1), the National Natural Science Foundation of China (no. 10632020), the German Academic Exchange Service (DAAD, Project-no. D/08/01795) and the China Scholarship Council (CSC) are gratefully acknowledged.

Appendix A. The wavelet method

In this appendix, the wavelet method for Eqs. (1) and (2) is presented. For convenience and without loss of generality, Eqs. (1) and (2) may be rewritten as follows

$$\frac{\partial^2}{\partial x^2}\left[\alpha_1(x)\frac{\partial^2 u(x,t)}{\partial x^2}\right]+\frac{\partial}{\partial x}\left[\alpha_2(x)\frac{\partial u(x,t)}{\partial x}\right]+\alpha_3(x)\frac{\partial^2 u(x,t)}{\partial t^2}=0, \tag{A.1}$$

where $\alpha_i(x)$ $(i=1,2,3)$ are periodic functions of the variable x denoting EI, EIb, and ρA in Eqs. (1) and (2) with the purely elastic periodic beam ($b=0$) and the piezoelectric one ($b\neq 0$), and $u(x,t)$ is the displacement in y-direction.

For a periodic structure, Bloch's theorem asserts that the time-harmonic solution $u(x,t)$ to Eq. (A.1) can be written as

$$u(x,t)=\mathrm{e}^{\mathrm{i}(kx-\omega t)}u_k(x), \tag{A.2}$$

where ω is the angular frequency, k is restricted within the first Brillouin-zone (BZ) $[-\pi/a,\pi/a]$ of the reciprocal lattice, and $u_k(x)$ is a function with the same periods $\alpha_i(x)$, which can be expanded in the form of bior1.1 wavelets and scaling functions as [10]

$$f(x)=\sum_{n\in Z}s_n\varphi_{j_0,n}^{\mathrm{bior1.1}}(x)+\sum_{\substack{j\in Z\\ j\geq j_0}}\sum_{n\in Z}d_{j,n}\psi_{j,n}^{\mathrm{bior1.1}}(x), \tag{A.3}$$

$$u_k(x)=\sum_{b_m\in\Psi_{j_0,J}}\tilde{u}_{k,m}b_m, \tag{A.4}$$

where $f(x)$ stands for EI, EIb, and ρA, respectively; $s_n=\langle\psi_{j_0,n}^{\mathrm{bior1.1}},f\rangle$ and $d_{j,n}=\langle\psi_{j,n}^{\mathrm{bior1.1}},f\rangle$ are the wavelet coefficients; the set $\Psi_{j_0,J}$ is given by

$$\{\varphi_{j_0,n}:n=0,\ldots,2^{j_0}-1\}\cup\{\psi_{j,n}:n=0,\ldots,2^j-1,j=j_0,\ldots\infty,J-1\}.$$

Each function in this set is the wavelet and the scaling functions. The integer J determines the approximation degree as well as the maximum number 2^J of the wavelets and the scaling basis functions used in the expansion.

According to the variational principle, Eq. (A.1) can be recast into the following integral form

$$\int_\Omega \alpha_1(x)\left(\frac{\partial}{\partial x}+\mathrm{i}k\right)^2 u_k\cdot\overline{\left(\frac{\partial}{\partial x}+\mathrm{i}k\right)^2 v}\,\mathrm{d}x+\int_\Omega\alpha_2(x)\left(\frac{\partial}{\partial x}+\mathrm{i}k\right)u_k\cdot\overline{\left(\frac{\partial}{\partial x}+\mathrm{i}k\right)v}\,\mathrm{d}x=\omega^2\int_\Omega\alpha_3(x)u_k\bar{v}\,\mathrm{d}x \tag{A.5}$$

where v is an arbitrary square integrable function, and substituting Eqs. (A.2) and (A.4) into Eq. (A.5), we obtain

$$\mathbf{A}_k\tilde{\mathbf{u}}_{k,m}=\omega^2\mathbf{B}_k\tilde{\mathbf{u}}_{k,m}, \tag{A.6}$$

where $\mathbf{A}_k$ and $\mathbf{B}_k$ are sparse matrices and $\tilde{\mathbf{u}}_{k,m}$ is the displacement vector. This leads to an eigenvalue problem of a $2^{J+1}\times 2^{J+1}$ matrix. The matrix elements are given by

$$(\mathbf{A}_k)_{p,q}=\int_\Omega\alpha_1(x)\left(\frac{\partial}{\partial x}+\mathrm{i}k\right)^2 b_p\overline{\left(\frac{\partial}{\partial x}+\mathrm{i}k\right)^2\tilde{b}_q}\,\mathrm{d}x+\int_\Omega\alpha_2(x)\left(\frac{\partial}{\partial x}+\mathrm{i}k\right)b_p\cdot\overline{\left(\frac{\partial}{\partial x}+\mathrm{i}k\right)\tilde{b}_q}\,\mathrm{d}x, \tag{A.7}$$

$$(\mathbf{B}_k)_{p,q} = \int_{\Omega} \alpha_3(x) b_p \tilde{b}_q \, dx. \tag{A.8}$$

Using the bior1.1 wavelet expansion (A.3) for the functions *EI*, *EIb*, and ρA, Eqs. (A.7) and (A.8) are transformed into the calculation of a linear combination of the wavelets integrals, for more mathematical details see for instance Ref. [10]. Eq. (A.6) is an infinite set of linear equations. In practice, only a finite number of wavelet basis functions are employed in the calculation. We employ 128 wavelets in this paper and the convergence of the method is ensured.

References

[1] J.D. Joannopoulos, R.D. Meade, J.N. Winn, *Photonic Crystals*, Princeton University Press, Princeton, NJ, 1995.
[2] D.J. Mead, S. Markus, Coupled flexural–longitudinal wave motion in a periodic beam, *Journal of Sound and Vibration* 90 (1983) 1–24.
[3] M.S. Kushwaha, P. Halevi, G. Martinez, L. Dobrzynski, B. Djafari-Rouhani, Theory of acoustic band structure of periodic elastic composites, *Physical Review B* 49 (1994) 2313–2322.
[4] D. Richards, D.J. Pines, Passive reduction of gear mesh vibration using a periodic drive shaft, *Journal of Sound and Vibration* 264 (2003) 317–342.
[5] J.H. Wen, G. Wang, D.L. Yu, H.G. Zhao, Y.Z. Liu, Theoretical and experimental investigation of flexural wave propagation in straight beams with periodic structures: application to a vibration isolation structure, *Journal of Applied Physics* 97 (2005) 114907.
[6] O. Thorp, M. Ruzzene, A. Baz, Attenuation and localization of wave propagation in rods with periodic shunted piezoelectric patches, *Smart Materials and Structures* 10 (2001) 979–989.
[7] A.L. Chen, F.M. Li, Y.S. Wang, Localization of flexural waves in a disordered periodic piezoelectric beam, *Journal of Sound and Vibration* 304 (2007) 863–874.
[8] Y.Z. Liu, D.L. Yu, L.H.G. Zhao, J.H. Wen, X.S. Wen, Design guidelines for flexural wave attenuation of slender beams with local resonators, *Physics Letters A* 362 (2007) 344–347.
[9] Z.Y. Liu, X.X. Zhang, Y.W. Mao, Y.Y. Zhu, Z.Y. Yang, C.T. Chan, P. Sheng, Locally resonant sonic materials, *Science* 289 (2000) 1735.
[10] Z.Z. Yan, Y.S. Wang, Wavelet-based method for computing elastic band gaps of one-dimensional phononic crystals, *Science in China Series G: Physics Mechanics and Astronomy* 50 (2007) 622–630.
[11] F.M. Li, Y.S. Wang, C. Hu, W.H. Hang, Wave localization in randomly disordered periodic layered piezoelectric structures, *Acta Mechanic Sinica* 22 (2006) 559–567.
[12] D.L. Yu, J.H. Wen, H.G. Zhao, Y.Z. Liu, X.S. Wen, Vibration reduction by using the idea of phononic crystals in a pipe-conveying fluid, *Journal of Sound and Vibration* 318 (2008) 193–205.
[13] J.S. Jensen, Phononic band gaps and vibrations in one- and two-dimensional mass-spring structures, *Journal of Sound and Vibration* 266 (2003) 1053–1078.
[14] C. Goffaux, J. Sánchez-Dehesa, A. Levy Yeyati, P. Lambin, A. Khelif, J.O. Vasseur, B. Djafari-Rouhani, Evidence of Fano-like interference phenomena in locally resonant materials, *Physical Review Letters* 88 (2002) 225502.